Proceedings of ISINN-29, JINR, E3-2023-58, Dubna, 2023, p.75 – 87

Measurement of Cross Sections for Nuclear Reactions of Interaction of Protons and Deuterons with Lithium at Ion Energies 0.4 – 2.2 MeV

Bikchurina M., Bykov T., Kasatov D., Kolesnikov I., Koshkarev A., Ostreinov G., Savinov S., Sokolova E., and Taskaev S.

Budker Institute of Nuclear Physics, Novosibirsk, Russia
Novosibirsk State University, Novosibirsk, Russia

An accelerator based epithermal neutron source for the development of boron neutron capture therapy (BNCT), a promising method for the treatment of malignant tumors, and other various applications is proposed, created and is functioning at the Budker Institute of Nuclear Physics. The neutron source consists of a tandem accelerator of charged particles of an original design, a lithium neutron-generating target for generating neutrons as a result of the ^{7}Li(p,n)^{7}Be or ^{7}Li(d,n) reaction, and a beam shaping assembly for forming a therapeutic beam of epithermal neutrons. The facility is capable of producing α-particles through different reactions.

Knowledge of the cross sections of the reactions Li(p,), Li(d,) is important both for nuclear data evaluation, as well as within the framework of BNCT and other applications. In this work, the cross sections of the following nuclear reactions were determined with good accuracy for proton/deuteron energies E = 0.4–2.2 MeV: ^{7}Li(d,nα)^{4}He, ^{7}Li(d,α)^{5}He →α + n, ^{6}Li(d,α)^{4}He, ^{6}Li(d,p)^{7}Li, ^{6}Li(d,p)^{7}Li*, ^{7}Li(p,α)^{4}He. The measurements were made using a silicon-based semiconductor α-spectrometer by ion scattering spectroscopy. The energy distribution of alpha particles from a thick layer of boron carbide when irradiated with a proton beam with energies from 0.6 to 2.1 MeV was measured. The results show that it is possible to measure the cross sections of the nuclear reactions ^{11}B(p,α)^{8}Be and ^{11}B(p,α)αα using the thin boron layer. For the deposition of a thin layer of boron on a metal substrate it is proposed to carry out a magnetron sputtering method with preheating of the thermally insulated target by a low-current high-voltage discharge. Measurement of the reaction cross section is important for both boron-proton-capture therapy and for neutron-free thermonuclear energy on the ^{11}B(p,α)αα reaction.

1. Introduction

The prevalence of cancer and mortality rates are steadily increasing. Boron-neutron capture therapy (BNCT) is considered one of the promising approaches for treating malignant tumors [1,2]. BNCT is a form of binary radiotherapy, when the stable isotope boron-10 is accumulated in tumor cells using special pharmaceuticals and then irradiated with a stream of epithermal neutrons (0.5 eV– 10 keV). As a result of neutron capture by the atomic nucleus boron-10 (thermal neutron capture cross-section 3838 barns) the nuclear reaction ^{10}B(n,α)^{7}Li with energy release of 2.79 MeV occurs. This therapy has already been validly used in clinical trials to treat patients and has shown positive results.

Charged-particle accelerators are now used as neutron sources. The Budker Institute of Nuclear Physics SB RAS proposed and created [3] a VITA, which includes i) a tandem electrostatic accelerator of charged particles of original design (vacuum-insulated tandem accelerator) to produce a monoenergetic beam of protons or deuterons with energy from 0.3 to 2.3 MeV, current up to 10 mA, (ii) a thin lithium target to generate a powerful neutron flux in the ^{7}Li(p,n)^{7}Be and Li(d,n) reactions, (iii) beam forming systems to produce a beam of cold, thermal, epithermal or fast neutrons. The facility is equipped with gamma, alpha, and neutron spectrometers and dosimeters.

The interaction of a proton with lithium is also accompanied by the reaction $^{7}Li(p,\alpha)^{4}He$. This reaction is characterized by an energy yield of 14.347 MeV and is one of the thermonuclear reactions in stars. Existing data on the cross section of the reaction are very inconsistent; one of the goals of this work is to measure the cross section of the $^{7}Li(p,\alpha)^{4}He$ reaction.

As noted above, VITA can generate not only a beam of protons but also deuterons, so the second goal of this work is to study the interaction between lithium and deuterons, since this issue is poorly understood.

In addition to the $^{7}Li(p,\alpha)^{4}He$ reaction, the $^{11}B(p,\alpha)\alpha\alpha$ reaction is often considered for neutron-free fusion. In addition to the fundamental application, this reaction appears in the BNCT, which emphasizes the importance of studying the cross section of the interaction between boron-10 and proton. At the present time the cross sections of the interaction of natural boron with a proton are poorly studied, our goal was to study the nature of the interaction of boron with the proton beam.

2. Experimental facility

The study was carried out on an accelerator-based neutron source at the Budker Institute of Nuclear Physics in Novosibirsk, Russia [2]. A schematic of the experimental setup is shown in Figure 1. The vacuum-insulated tandem accelerator *1* produces a proton beam and directs it toward the lithium target *6*. The proton beam energy can be varied in the range of 0.6–2 MeV, maintaining a high energy stability of 0.1%. The beam current can also be varied in the range from 0.5 to 10 mA, ensuring its stability of 0.4%. At the VITA exit the proton beam has a transverse size of 10 mm, angular divergence up to ± 1.5 mrad, and a normalized emittance of 0.2 mm-mrad [4]. The proton beam current is measured and monitored with a non-contact NPCT current sensor (Bergoz Instrumentation, France) *2*.

In order to conduct research, the proton beam current on the target is reduced to less than 1.5 μA by placing a cooled collimator *2* in its path located 4 m from the target. The collimator is a 16 mm thick copper rectangular parallelepiped with sides 64 × 64 mm. A 1 mm diameter hole is drilled in the center of the aperture and a 10 mm countersink is made on both sides.

The position and size of the proton beam on the target is monitored by a Hikvision video camera *5*, which records the lithium luminescence under the action of protons [5]. The current of the proton beam falling on the lithium target is measured with a resistive voltage divider, using a target assembly *4* electrically isolated from the setup, like a deep Faraday cylinder.

The developed lithium target *6* is three-layered: a thin layer of pure lithium metal for neutron generation, a thin layer of material for proton absorption, and a thin copper substrate for efficient heat dissipation. The copper substrate is a 144 mm diameter copper disk with a thickness of 8 mm. On the proton beam side, an 84 mm diameter thin layer of lithium crystal density is thermal sprayed on the copper disk. A flat aluminum disk with a hole in the center for the supply of cooling water and two holes on the periphery for water drainage is clamped to the back side of the copper disk.

In scientific research, target assemblies with two or three spigots, angled 135°, 142.5°, or 168° to the beam axis, are used to observe or place diagnostic equipment.

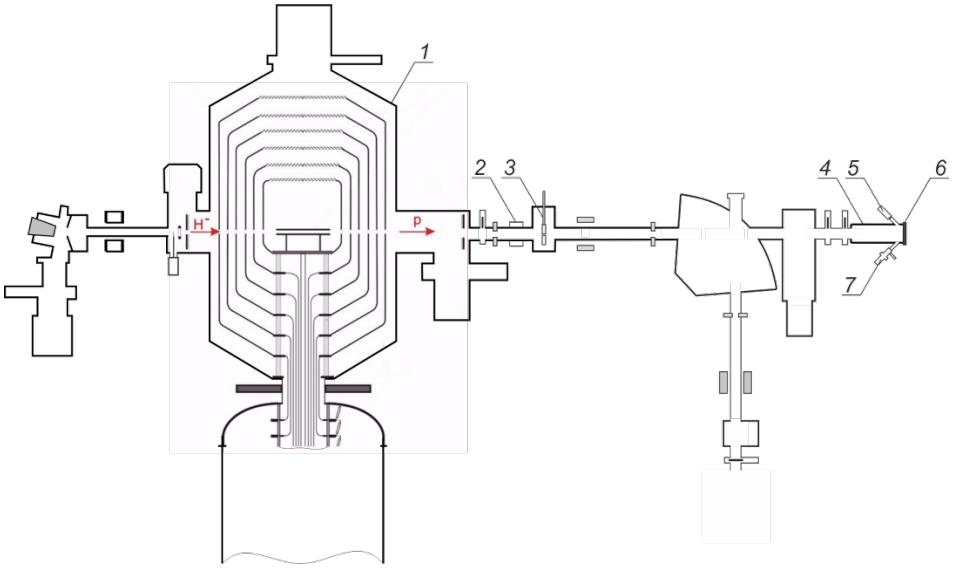

Figure 1 – Scheme of the experimental facility: *1* – vacuum insulated tandem accelerator, *2* – non-destructive DC current transformer, *3* – collimator, *4* – target assembly, *5* – video camera, *6* – lithium target, *7* – α-spectrometer.

The intensity and energy of α-particles are measured by an α-spectrometer *7* with a PDPA 1K silicon semiconductor detector (Institute of Physical and Technical Problems, Dubna, Russia). The area of the sensitive detector surface S = 20 mm^2, energy resolution – 13 keV, noise energy equivalent – 7 keV, capacity – 30 pF, input window thickness – 0.08 μm, standard natural background in the 3–8 MeV range – 0.15 imp/(cm^2·h).

3. Results and discussion

3.1. Measurement of cross section of ^{7}Li(p,α)^{4}He reaction

The ^{7}Li(p,α)^{4}He reaction is characterized by a high energy yield of 14.347 MeV and is one of the thermonuclear reactions involved in the stellar cycle of heavy element fusion in the universe [6]. This reaction also accompanies the generation of neutrons in the ^{7}Li(p,α)^{4}He reaction, which is used in a number of neutron sources [7] for boron-neutron capture therapy of malignant tumors [1,2,8]. Knowing the cross section of the ^{7}Li(p,α)^{4}He reaction is certainly important for evaluating nuclear data. However, the existing cross-section data sets in the literature are, unfortunately, contradictory in many cases [9–19]. Figure 2 shows cross section data for the ^{7}Li(p,α)^{4}He reaction and differential cross section data for this reaction.

To measure the cross section of the reaction ^{7}Li(p,α)^{4}He at a certain time *t* by a beam of protons with a current *i*, a lithium layer of thickness *l* is irradiated and α-spectrometer records α-particles escaping at a solid angle $\Omega_{lab} = S/R^2 = 7{,}511 \cdot 10^{-5}$, R = 516 mm, at an angle 168 ± 0,5° to the proton momentum. To measure the cross section, in addition to the library values, it is necessary to know the efficiency of the α-spectrometer, the thickness of the lithium layer, the nuclear density ^{7}Li in the lithium layer, the solid angle and the proton fluence.

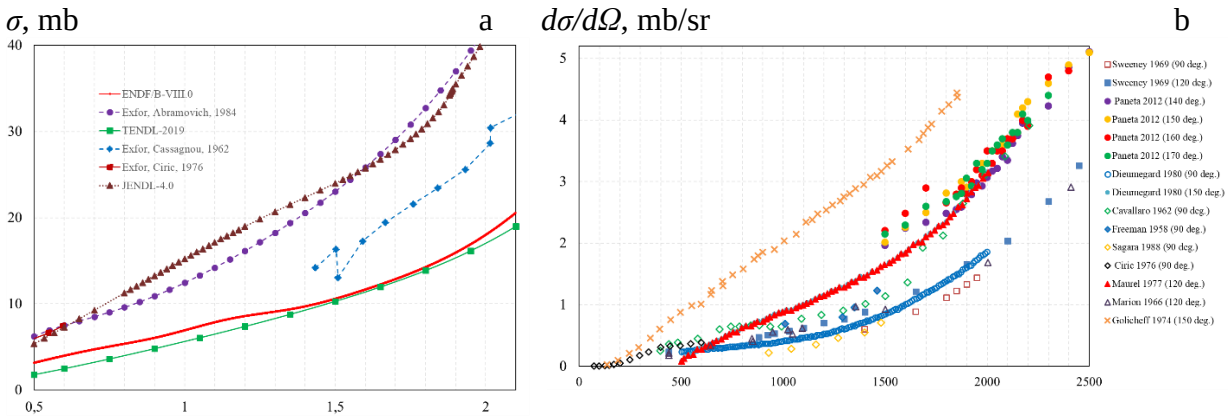

Figure 2 – a) Cross section data for the ^{7}Li(p,α)^{4}He reaction presented in the Java based nuclear information software JANIS v.3.0 [9]. b) Differential cross section of the ^{7}Li(p,α)^{4}He reaction.

The efficiency of the α-spectrometer was calibrated using two reference radiation sources based on the radionuclide plutonium-239 and a reference spectrometric α-source with the isotope ^{226}Ra and is equal to 100%. The nuclear density of ^{7}Li was calculated based on the lithium passport data and is $4.251 \cdot 10^{22}$cm^{-3} with an accuracy of 0.1 % [20–22]. Special attention was paid to the determination of the thickness of the lithium layer; for this purpose the most precise method was used – the method of comparing the yield of 478 keV γ-quanta from the examined lithium layer and from the thick layer irradiated with 1.85 MeV protons (Figure 3). We call the thick layer the lithium layer thicker than the proton path length in lithium to the reaction threshold energy ^{7}Li(p,p′γ)^{7}Li, equal to 478 keV [23]. The thickness is calculated using an expression of the proton energy loss rate in lithium as a function of its energy:

$$S = \frac{S_{low} \cdot S_{high}}{S_{low} + S_{high}} \text{ eV}/(10^{15}\text{at/cm}^2), \quad (1)$$

where $S_{low} = 1{,}6E^{0{,}45}$, $S_{high} = \frac{725{,}6}{E}\ln(1 + \frac{3013}{E} + 0{,}04578E)$, E in keV.
Thus, the thickness of lithium is l = 0.422 ± 0,013 μm.

When measuring the cross section of the ^{7}Li(p,α)^{4}He reaction, the sensitive part of the α-spectrometer detector is placed at a distance of 516 mm from the lithium at an angle of 168 ± 0.5° to the proton impulse. The characteristic spectrum recorded by the α-spectrometer is shown in Figure 3. The main signal (*1*, *2*, and *3* in Figure 4a) are protons backscattered on copper atomic nuclei, with *1* being single events, *2* being double events, and *3* being triple events. Against this background of single events, small peaks due to proton scattering on atomic nuclei of lithium, carbon, and oxygen (Li, C, and O in Figure 4b) stand out clearly. The lithium target was previously found to be covered by a thin layer of lithium oxide (10–50 nm) and a carbon film (0.5–2 nm). The back-scattered proton spectrum simulated by SIMNRA v.7.03 [24] with the above thickness of lithium, carbon and oxygen layers agrees well with that measured. Signal *4* is α-particle, signal *5* is events of simultaneous registration α-particle and back-scattered proton.

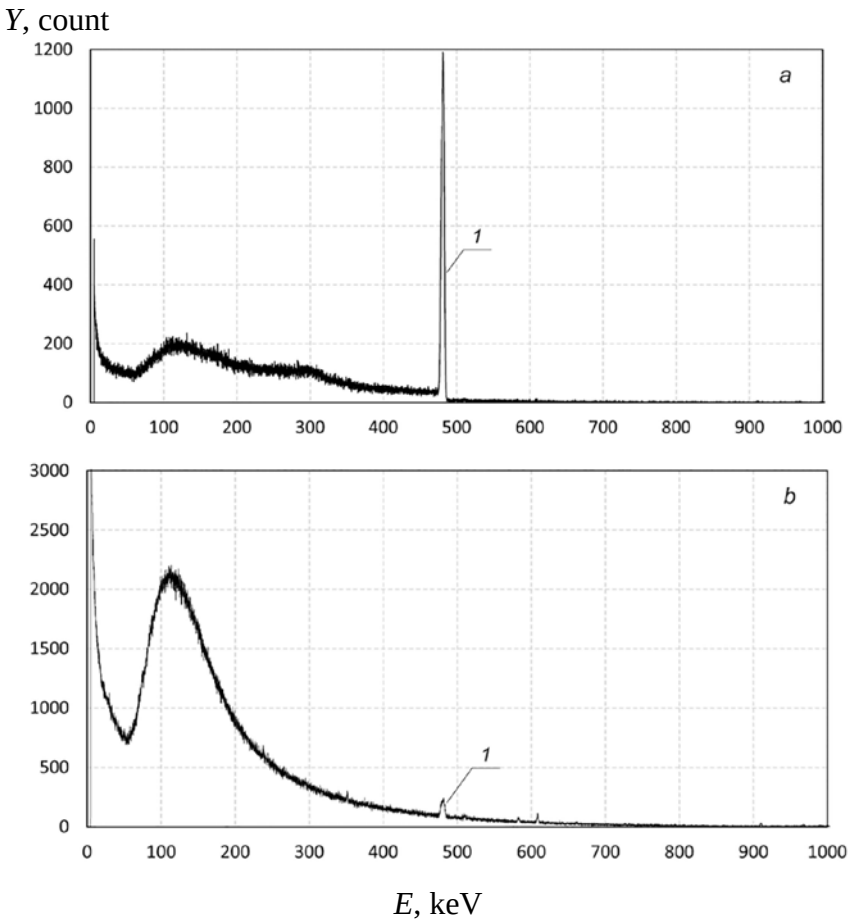

Figure 3 – Spectrum from HPGe γ-spectrometer: *a* – thick lithium layer, *b* – thin lithium layer.

The energy of α-particles depends on the energy of protons; let us determine this dependence. When a proton collides with a stationary lithium nucleus, a short-lived ($\tau \sim 10^{-18}$ s) compound nucleus is formed, which acquires momentum and, moving, decays into two α-particles. As the proton energy increases, the energy of the α-particle emitted at an angle 168° to the proton momentum decreases. Thus, if at the proton energy of 1 MeV the energy of the α-particle is 7.663 MeV, then at 2 MeV it is 7.523 MeV.

Maximums in the measured energy distributions of α-particles are obtained at energies lower than the calculated ones by 50–70 keV. Such a shift may be caused by ionization losses of the α-particle while passing through the lithium layer. According to the Bethe-Bloch formula [26], the ionization losses of the α-particle in lithium are ≈ 600 MeV/(g·cm^2), and the α-particle loses energy of ≈ 134 keV while passing a 0.422 μm thick lithium layer. Since α-particles are generated throughout the lithium thickness, on average they pass through 0.211 μm lithium and their average energy loss is 67 keV which agrees well with the measured energy shift. Consequently, the measured energy shift of the α-particle is due to its ionization losses as it passes through the lithium layer.

The measurements were made at 10 energy values. The cross section data obtained are presented in the tables in [29] and in Figure 5 and 6 in comparison with data from other authors and nuclear reaction databases. It can be seen that the values of the differential reaction cross section we obtained are in agreement with most of the Ciric [16] data measured at 90˚ and differ from the rest of the data. Our full cross section data are in good agreement

with the Abramovich data and the data in the JENDL 4.0 database [27]. It can be noted that our data on the cross section with good accuracy are exactly 2 times higher than the values presented in ENDF/B-VIII.0. We cannot explain such significant discrepancies in the data of different authors.

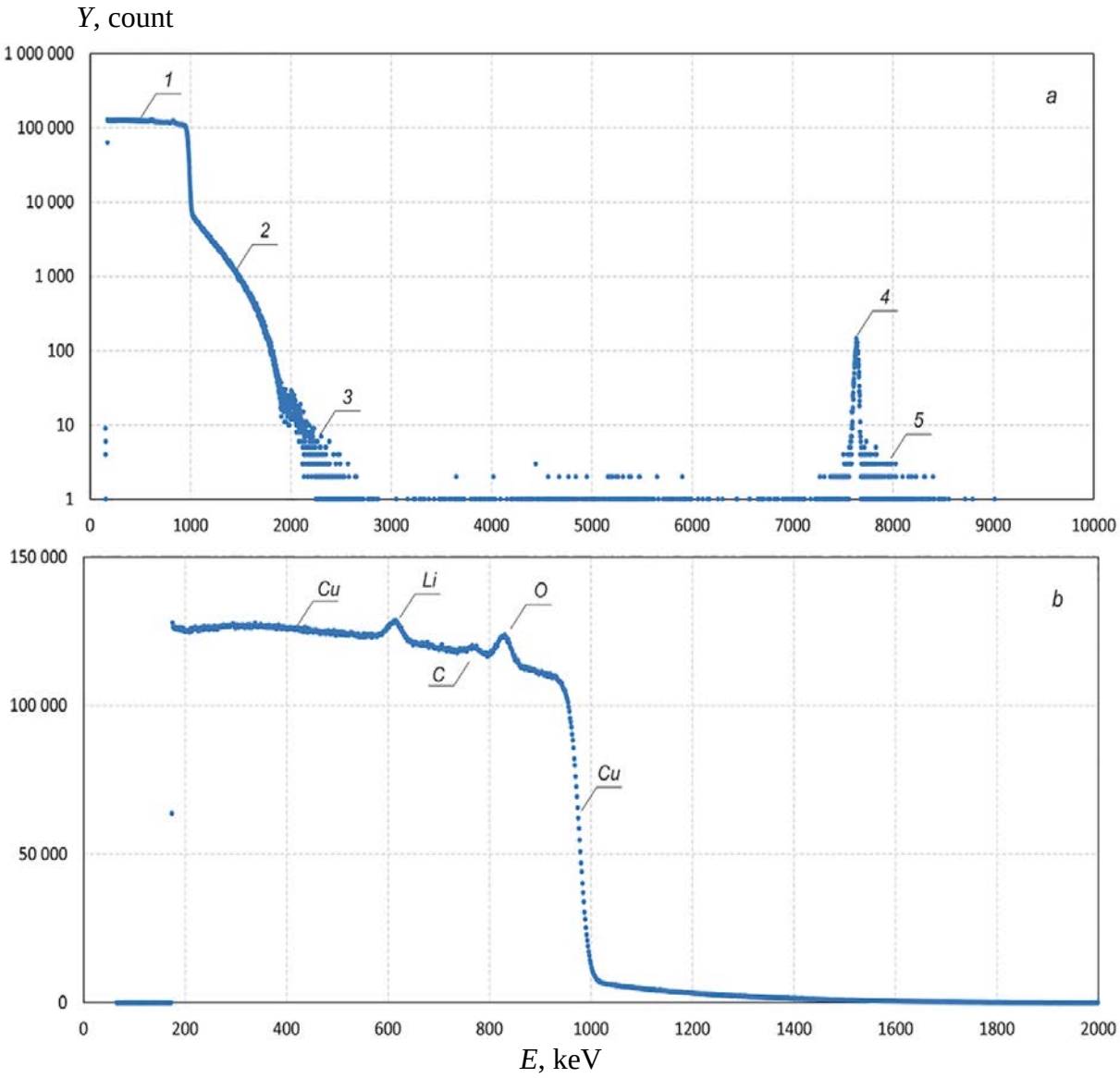

Figure 4 – Spectrum of charged particles recorded by α-spectrometer at proton energy 1 MeV: *1–3* – back-scattered protons from copper atoms (*1* – single events, *2* – double, *3* – triple), *4* – α-particles, *5* – simultaneous registration α-particle and proton. Cu, Li, C, and O – back-scattered protons from copper, lithium, carbon, and oxygen atoms.

The values of the $^{7}Li(p,\alpha)^{4}He$ reaction cross section we obtained were entered into the IBANDL (International Atomic Energy Agency Nuclear Data Library for Ion-Ray Analysis) and Exfor (experimental nuclear reaction data) databases [28].

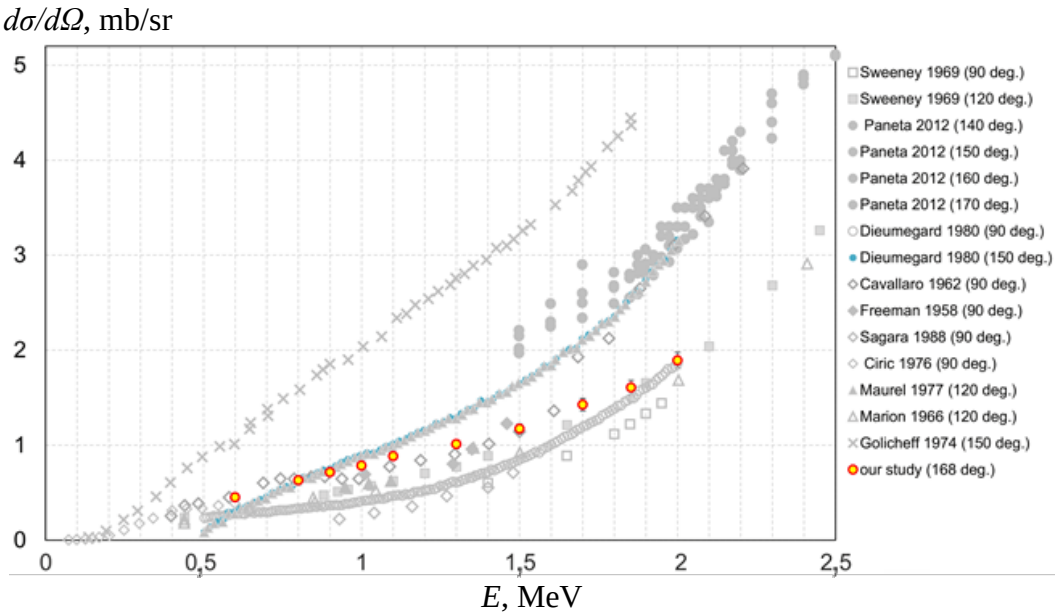

Figure 5 – Differential cross section of the ^{7}Li(p,α)^{4}He reaction.

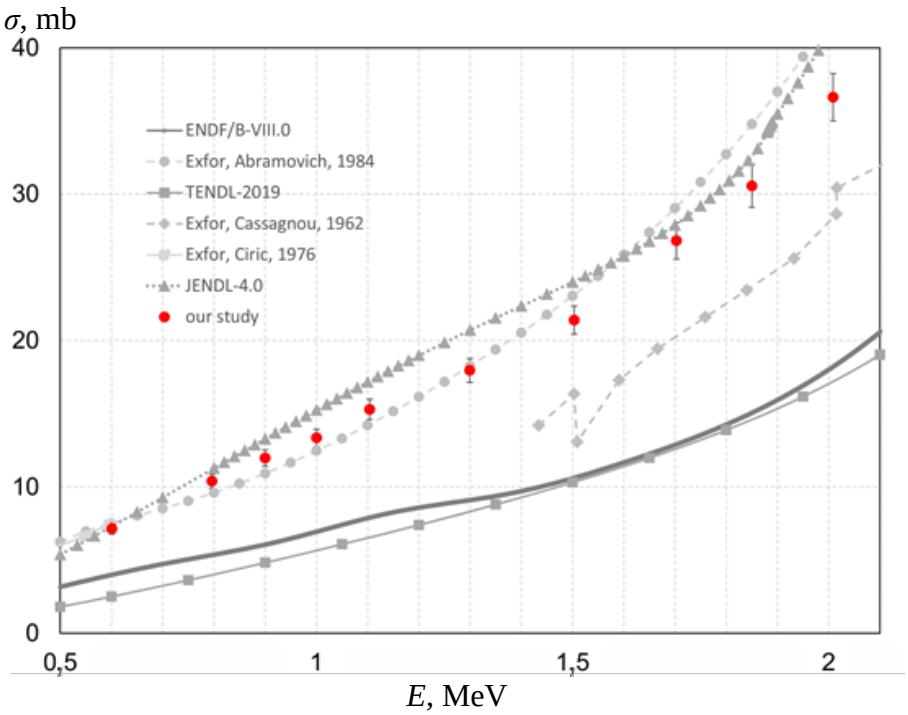

Figure 6 – Cross section of the ^{7}Li(p,α)^{4}He reaction.

3.2. Measurement of cross section of ^{7}Li(d,), ^{6}Li(d,) reactions

VITA generates both proton and deuteron beams. The interaction of deuterons with lithium is used to generate fast neutrons in the non-threshold reaction ^{7}Li(d,n)^{8}Be (Q = 15.028 MeV), the reaction products are actively used in testing various materials, including the needs of CERN and ITER, as well as in cancer therapy with fast neutrons, fundamental research and other applications. In addition to this reaction, the lithium target enters into a number of other different interactions with the deuteron beam: ^{16}O(d,p)^{17}O (Q = 1.917 MeV), ^{16}O(d,p)^{17}O*

(Q= 1.046 MeV), $^{16}O(d,\alpha)^{14}N$ (Q = 3.110 MeV), $^{12}C(d,p)^{13}C$ (Q = 2.722 MeV), $^{6}Li(d,p_1)^{7}Li^*$ (Q = 4.550 MeV), $^{6}Li(d,p_0)^{7}Li$ (Q = 5.028 MeV), $^{6}Li(d,\alpha)^{4}He$ (Q = 22.38 MeV), $^{6}Li(d,p\alpha)^{3}H$ (Q= 2.6 MeV), $^{6}Li(d, ^{3}He)^{5}He$ (Q= 0.840 MeV) $^{5}He = n + \alpha + 0.957$ MeV, $^{6}Li(d,t)^{5}Li$ (Q= 0.595 MeV), $^{6}Li(d,n)^{7}Be$ (Q = 3.385 MeV), $^{7}Li(d,n\alpha)^{4}He$ (Q= 15.121 MeV), $^{7}Li(d,\alpha)^{5}He$ (Q= 14.162 MeV) $^{5}He = n + \alpha + 0.957$ MeV, $^{7}Li(d,n)^{8}Be$ (Q = 15.028 MeV), $^{7}Li(d,n)^{8}Be^*$ (Q= 15.027 MeV) $^{8}Be^* = \alpha + \alpha + 0.095$ MeV. Data of the most submitted reactions are unclear and limited, examples are shown in Figures 7 and 8 [30–39].

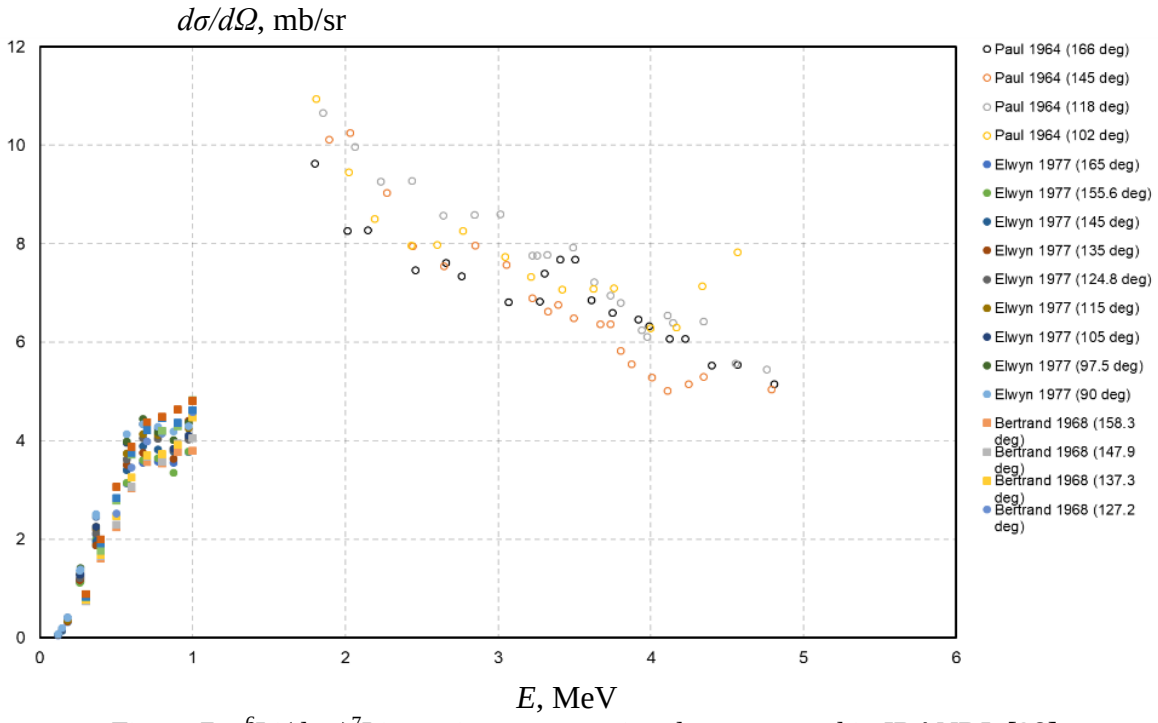

Figure 7 – $^{6}Li(d,p_0)^{7}Li$ reaction cross section data presented in IBANDL [28].

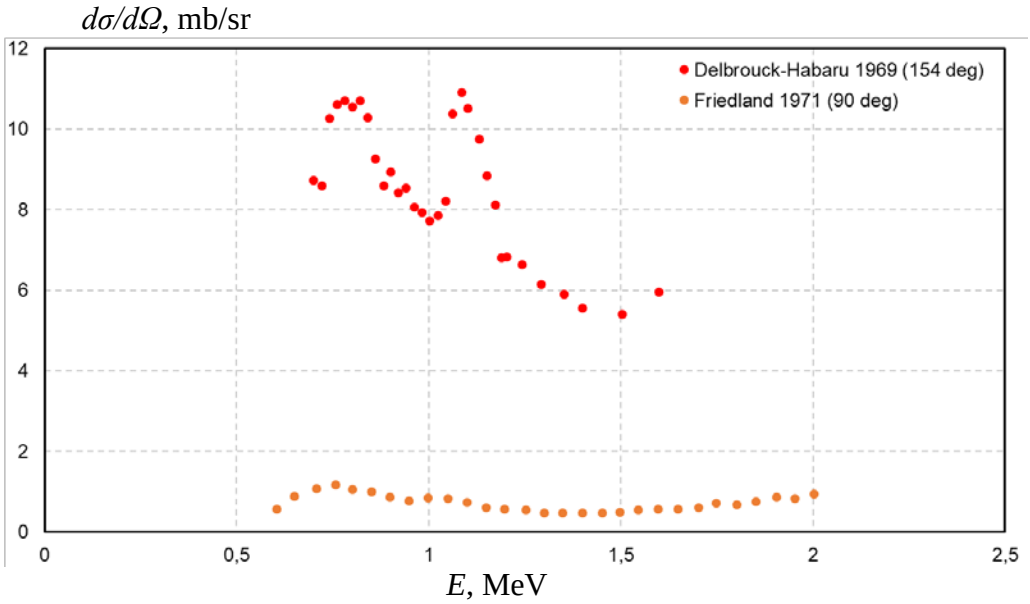

Figure 8 – $^{7}Li(d,\alpha)^{5}He$ reaction cross section data presented in IBANDL [28].

Measurements of the spectra of charged particles were carried out at a deuteron energy of 0.4-2.0 MeV in a geometry similar to the previous experiment, α-spectrometer was placed at a 135 ° angle to the beam axis, a thin lithium target (~ 2 μm) was used as a target. A detailed match of the detected reactions with the peaks in the spectrum is shown in Figure 9. We plan to measure the cross sections of the reactions presented under numbers 3-7 using VITA.

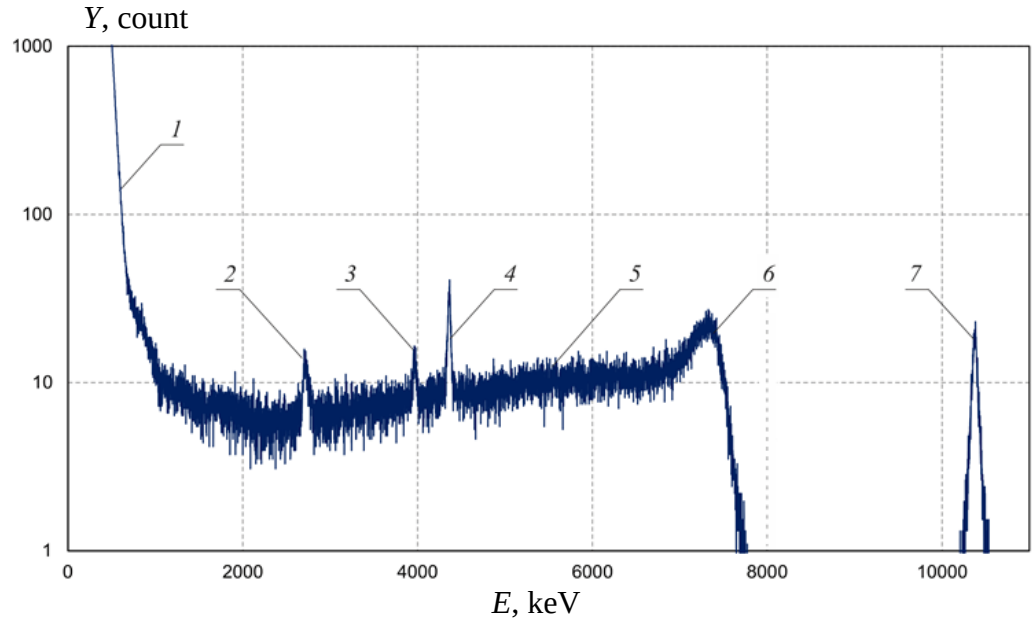

Figure 9 – Energy spectrum of charged particles detected by α-spectrometer at an angle 135° when irradiating a lithium target with 0.4 MeV deuterons: *1* – deuterons reflected from the target, *2* – reaction products of $^{16}O(d,\alpha)^{14}N$, *3* – $^{6}Li(d,p_1)^{7}Li^*$, *4* – $^{6}Li(d,p_0)^{7}Li$, *5* – $^{7}Li(d,n\alpha)^{4}He$ and decay of resulting ^{5}He, *6* – $^{7}Li(d,\alpha)^{5}He$, *7* – $^{6}Li(d,\alpha)^{4}He$.

3.3. Measurement of cross section of $^{11}B(p,\alpha)\alpha\alpha$ reaction

The reaction $^{11}B(p,\alpha)\alpha\alpha$ is characterized by an energy yield Q = 8.59 MeV and is one of the most promising as a basis for neutron-free fusion, in addition, boron is used in many other applications, including being present in the composition of drugs for BNCT, these and other applications of this reaction raises the question of knowing the exact cross section of interaction of boron with the proton beam. At this point, even the data on the progression of the proton reaction with boron-11 are controversial (Figures 10 and 11), suggesting that there are 4 possible routes: $^{11}B(p,\alpha)\alpha\alpha$, $^{11}B(p,\alpha_0)^{8}Be$, $^{11}B(p,\alpha_1)^{8}Be^*$, $^{11}B(p,\gamma)^{12}C$.

Measurements of charged particle spectra were carried out in a geometry similar to the previous experiment at proton energies of 0.4–2.15 MeV, α-spectrometer was placed at an angle of 135° to the beam axis, boron carbide (B_4C) was used as a target. The character of the proton energy dependence of the events is shown in Figure 12. One can see that as the energy increases, the right-hand peak corresponding to α_0 from the $^{11}B(p,\alpha_0)^{8}Be$ reaction increases with the proton energy, which coincides with the previously measured cross section of this boron-11-proton interaction route (Figure 10) [40–46]. One can also observe the complex character of the large peak, presumably formed by α_1 from the $^{11}B(p,\alpha_1)^{8}Be^*$ reaction, the decay of ^{8}Be and $^{8}Be^*$ into two α-particles, and the yield from the $^{11}B(p,\alpha)\alpha\alpha$ reaction. It is

still difficult to separate with certainty the contributions of the above reaction products on the spectrum. At this point, our team plans to further investigate the ^{11}B(p,α)αα reaction on a thin boron carbide target and eventually obtain a cross section of this reaction.

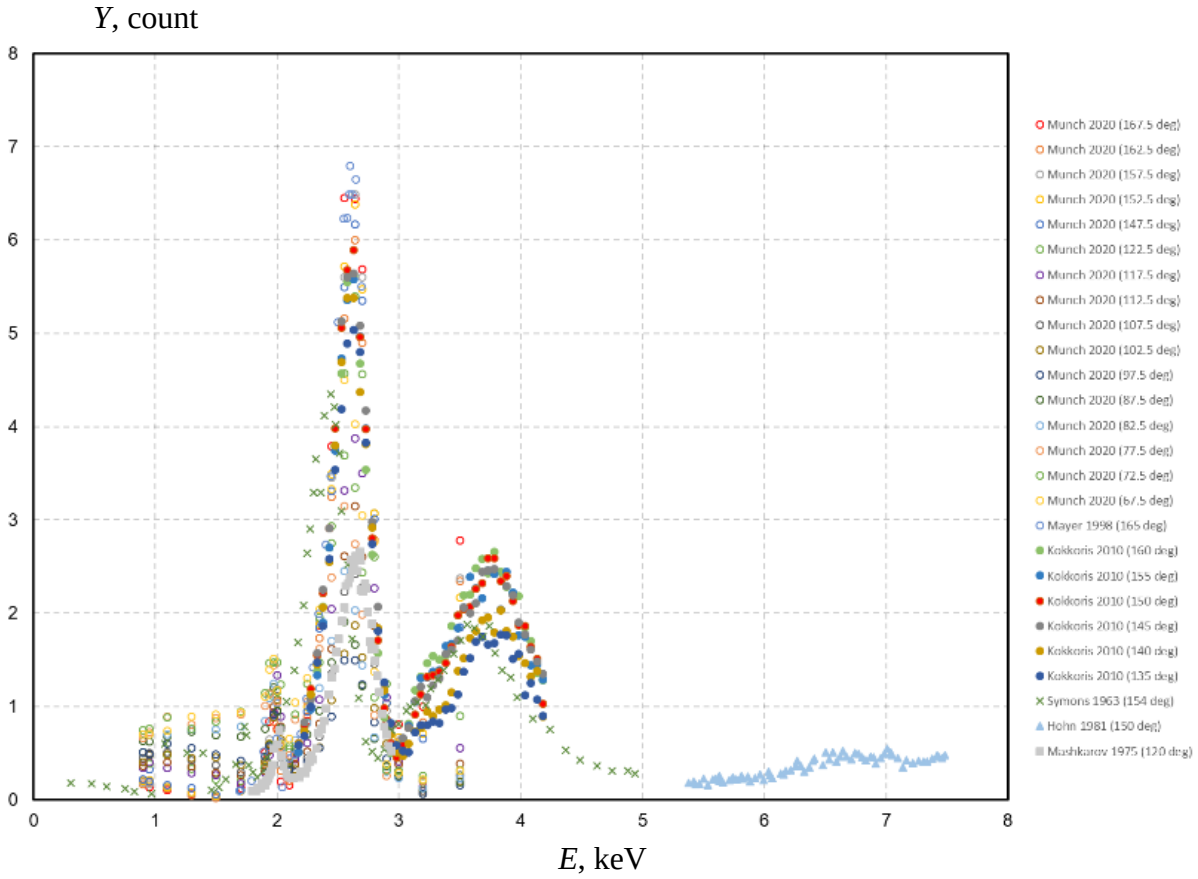

Figure 10 – ^{11}B(p,α_0)^{8}Be reaction cross section data presented in IBANDL [28].

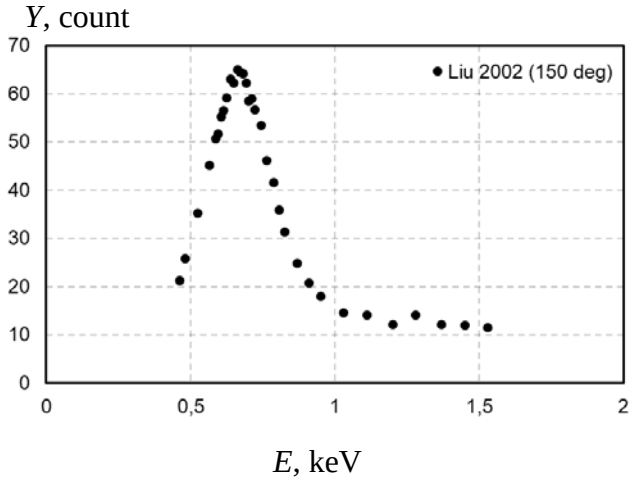

Figure 11 – ^{11}B(p,α_1)^{8}Be* reaction cross section data presented in IBANDL [28].

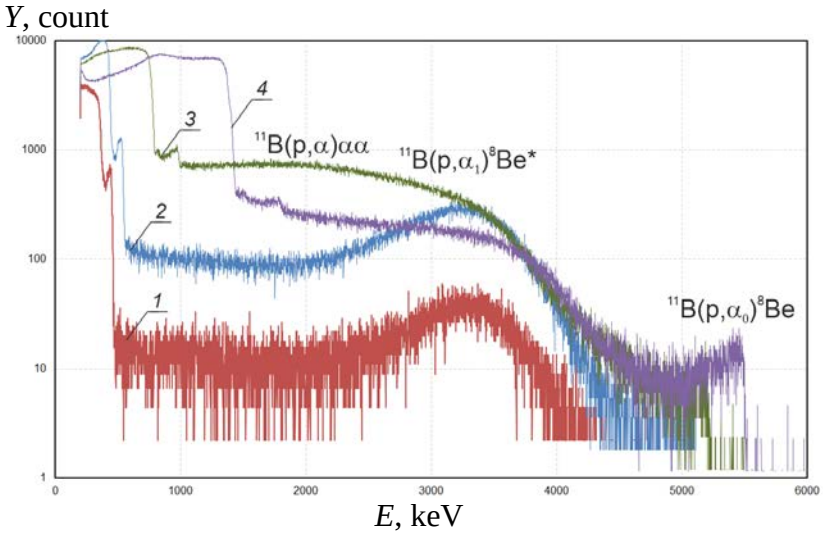

Figure 12 – Energy spectrum of charged particles detected by α-spectrometer at an angle 135° during the irradiation of boron carbide with protons with energy: *1* – 0.4 MeV, *2* – 0.5 MeV, *3* – 1.0 MeV, *4* – 2.0 MeV.

4. Conclusion

As a result of this study, the cross section of the $^{7}Li(p,\alpha)^{4}He$ reaction at proton energies from 0.6 MeV to 2 MeV was measured with high accuracy and precision. The high accuracy of the measurement was achieved by applying a new in situ method to measure the lithium thickness. The validity of this measurement is confirmed by agreement with the results of measurements made by five other independent methods: i) by measuring the mass of lithium deposited for sputtering, ii) by measuring the conductivity of water with which lithium was washed off the target copper substrate, iii) by the maximum shift in the energy distribution of α-particles, iv) by broadening the energy distribution of α-particles and v) by the energy distribution of back reflected protons on the lithium atomic nuclei.

The measured cross section of the $^{7}Li(p,\alpha)^{4}He$ nuclear reaction in the proton energy range of 0.6 MeV to 2 MeV was found to agree with the values given in the JENDL 4.0 nuclear reactions database and to be about 2 times greater than the values given in the ENDF/B VIII.0 and TENDL 2019 nuclear reactions databases.

The energy spectra of the reactions of lithium with deuterium $^{6}Li(d,p_1)^{7}Li^*$, $^{6}Li(d,p_0)^{7}Li$, $^{7}Li(d,n\alpha)^{4}He$, $^{7}Li(d,\alpha)^{5}He$, $^{6}Li(d,\alpha)^{4}He$ were measured and analyzed. An analysis of the character of the boron-11 reaction interaction with the proton was performed $^{11}B(p,\alpha)\alpha\alpha$.

Funding

This research was funded by Russian Science Foundation, grant number 19-72-30005, https://rscf.ru/project/19-72-30005.

References

1. W.A.G. Saurwein, A. Wittig, R. Moss, Y. Nakagawa (Eds.), Neutron Capture Therapy: Principles and Applications, Springer, 2012, https://doi.org/10.1007/ 978-3-642-31334-9.

2. S. Taskaev, V. Kanygin. Boron-Neutron Capture Therapy. Novosibirsk: SB RAS Publishing House, 2016. – p. 216.
3. Neutron Source Based on Vacuum Insulated Tandem Accelerator and Lithium Target / S. Taskaev, E. Berendeev, M. Bikchurina [et al.]. Biology. – 2021. – Vol. 10, nr 5. – P. 350. URL: https://doi.org/10.3390/biology10050350. – Дата публикации: 21.04.2021.
4. M. Bikchurina, T. Bykov, Ia. Kolesnikov, A. Makarov, G. Ostreinov, S. Savinov, S. Taskaev, I. Shchudlo. Measuring the Phase Portrait of an Ion Beam in a Tandem Accelerator with Vacuum Insulation. Instruments and Experimental Techniques, 2022, Vol. 65, No. 4, pp. 551–561.
5. Makarov, E. Sokolova, S. Taskaev. The luminescence of a lithium target under irradiation with a proton beam. Instruments and Experimental Techniques, 2021, Vol. 64, No. 1, pp. 24–27.
6. Tables of Physical Constants, Handbook. I.K. Kikoin Edition, AtomIzdat, Moscow (1976).
7. S. Taskaev, Development of an accelerator-based epithermal neutron source for boron neutron capture therapy, Phys. Part. Nucl. 50 (2019) 569–575, https://doi. org/10.1134/S1063779619050228.
8. IAEA-TECDOC-1223. Current Status of Neutron Capture Therapy. International Atomic Energy Agency, Vienna, 2001.
9. Java-based nuclear information software JANIS.
10. W. Sweeney, J. Marion, Gamma-ray ransitions involving isobaric-spin mixed states in Be^{8}, Phys. Rev. 182 (1969) 1007–1021, https://doi.org/10.1103/ PhysRev.182.1007.
11. V. Paneta, A. Kafkarkou, M. Kokkoris, A. Lagoyannis, Differential cross-section measurements for the $^{7}Li(p,p_0)^{7}Li$, $^{7}Li(p,p_1)^{7}Li$, $^{7}Li(p,\alpha_0)^{4}He$, $^{19}F(p,p_0)^{19}F$, $^{19}F(p,a_0)^{16}O$ and $^{19}F(p,\alpha_{1,2})^{16}O$ reactions, Nucl. Instrum. Methods Phys. Res. B. 288 (2012) 53–59, https://doi.org/10.12681/hnps.2492.
12. D. Dieumegard, B. Maurel, G. Amsel, Microanalysis of Flourine by nuclear reactions, Nucl. Instrum. Methods 168 (1-3) (1980) 93–103.
13. S. Cavallaro, R. Potenza, A. Rubbino, Li^{7}+p interaction and excited states of Be^{8}, Nucl. Phys. 36 (1962) 597–614, https://doi.org/10.1016/0029-5582%2862% 2990486-8.
14. J. Freeman, R. Hanna, J. Montague, The nuclear reaction $He^{4}(\alpha,p)Li^{7}$ and its inverse: II. The reaction $Li^{7}(p,\alpha)He^{4}$, Nucl. Phys. 5 (1958) 148–149, https://doi. org/10.1016/0029-5582(58)90013-0.
15. Sagara, K. Kamada, S. Yamaguchi, Depth profiling of lithium by use of the nuclear reaction $^{7}Li(p,\alpha)^{4}He$, Nucl. Instrum. Methods Phys. Res. B. 34 (1988) 465–469, https://doi.org/10.1016/0168-583X(88)90151-6.
16. D. Ciric, R. Popic, R. Zakula, B. Stepancic, M. Aleksic, J. Setrajcic, The interaction of ^{7}Li isotope with low energy proton and triton beams, Int. J. Sci. Res. 6 (1976) 115.
17. B. Maurel, D. Dieumegard, G. Amsel in Ion Beam Handbook (p. 133), ed. J. Mayer, E. Rimini, 1977, https://doi.org/10.1016/B978-0-12-480860-7.50011-3.
18. J. Marion, M. Wilson, The $^{7}Li(p,\gamma)^{8}Be^{*}$ reaction and single-particle levels in ^{8}Be, Nucl. Phys. 77 (1966) 129–148, https://doi.org/10.1016/0029-5582 (66) 90681-X.
19. Golicheff, M. Loeuillet, C.h. Engelmann, Determination des fonctions d'excitation des reactions $^{19}F(p,\alpha_0)^{16}O$ et $^{7}Li(p,\alpha_0)^{4}He$ entre 150 et 1800 keV: Application a la mesure des concentrations superficielles de lithium et de fluor, J. Radioanal. Chem. 22 (1–2) (1974) 113–129.

20. Method for in situ measuring the thickness of a lithium layer / D. Kasatov, Ia. Kolesnikov, A. Koshkarev [et al.]. – Текст : электронный // Journal of Instrumentation. – 2020. – Vol. 15. – P10006. – URL: https://doi.org/10.1088/1748-0221/15/10/P10006. – 12.10.2020.
21. Handbook of Stable Isotope Analytical Techniques. Volume II (2009) 1123–1321, doi:10.1016/B978-0-444-51115-7.00028-0.
22. Lieberman, G.J. Alexander, J.A. Sechzer, Stable isotopes of lithium: dissimilar biochemical and behavioral effects, Experientia 42 (9) (1986) 985–987, https:// doi.org/10.1007/BF01940701.
23. H. Andersen, J. Ziegler, Hydrogen stopping powers and ranges in all elements. Volume 3 of the stopping and ranges of ions in matter, Pergamon Press Inc., 1977.
24. SIMNRA v. 7.03 with SigmaCalc 2.0 for single user. License No. 1801-4848-WT- WA, Sept. 22, 2021.
25. Yu. Shirokov, N. Yudin, Nuclear Physics, Volumes 1 and 2, MIR Publishers, Moscow, 1982.
26. K.N. Mukhin. Experimental Nuclear Physics. - Moscow: Energoatomizdat, 1993.
27. JENDL – Japanese Evaluated Nuclear Data Library https://wwwndc.jaea.go.jp/jendl/jendl.html.
28. IBANDL – Ion Beam Analysis Nuclear Data Library https://www-nds.iaea.org/exfor/ibandl.htm.
29. S. Taskaev, M. Bikchurina, T. Bykov, D. Kasatov, Ia. Kolesnikov, A. Makarov, G. Ostreinov, S. Savinov, E. Sokolova. Cross-section measurement for the ^{7}Li(p, α)^{4}He reaction at proton energies 0.6–2 MeV. Nuclear Inst. and Methods in Physics Research B 525 (2022) 55–61.
30. J.M. Delbrouck-Habaru+(1969), Jour. Bull.Societe Royale des Sciences de Liege, Vol.38, p.240.
31. E. Friedland+(1971), Jour. Zeitschrift fuer Physik, Vol.243, Issue.2, p.126.
32. P. Paul+(1964), Jour. Nuclear Physics, Vol.53, Issue.3, p.465.
33. A.J. Elwyn+(1977), Jour. Physical Review, Part C, Nuclear Physics, Vol.16, p.1744.
34. F. Bertrand+(1968), Rept. Centre d`Etudes Nucleaires, Saclay Reports, No.3428.
35. B. Maurel,G.Amsel and D.Dieumegard, NIM, 191(1981), 349.
36. V. Foteinou et al., Nucl. Instr. and Meth. B 269, 2990 (2011).
37. F. Hirst+(1954), Jour. Philosophical Magazine, Vol.45, Issue.366, p.762.
38. G. Bruno+(1966), Jour. Journal de Physique, Vol.27, p.517.
39. G. Robaye+(1965), Jour. Bull.Societe Royale des Sciences de Liege, Vol.34, p.324.
40. M. Munch+(2020), European Physical Journal A: Hadrons and Nuclei, Vol.56, p.17.
41. M. Mayer et. al. Nucl. Instr. Meth. B143 (1998) 244.
42. M. Kokkoris+(2010), Jour. Nucl. Instrum. Methods in Physics Res., Sect.B, Vol.268, p.3539.
43. G.D. Symons and P.B.Treacy Nucl.Phys. v.46 (1963) 93.
44. K. Hohn+(1981), Jour. Jour. of Physics, Part G (Nucl.and Part.Phys.), Vol.7, p.803.
45. Ju.G. Mashkarov+(1975), Jour. Izv. Rossiiskoi Akademii Nauk, Ser.Fiz., Vol.39, p.1736.
46. J. Liu+(2002), Jour. Nucl. Instrum. Methods in Physics Res., Sect.B, Vol.190, p.107.